



OPEN

## Anatomical evaluations of the adipose tissue surrounding the flexor hallucis longus tendon

Tatsuhito Kawada<sup>1,2</sup>, Yasushi Shinohara<sup>3</sup>✉, Toshiyuki Kurihara<sup>4</sup>, Hayato Satake<sup>1</sup>, Kana Itokawa<sup>1</sup>, Masaki Fukuyoshi<sup>2</sup>, Norio Hayashi<sup>5</sup> & Katsumasa Sugimoto<sup>6</sup>

This study aimed to evaluate the presence of adipose tissue surrounding the flexor hallucis longus (FHL) tendon through gross dissection and magnetic resonance imaging (MRI). Grossly, we observed the FHL tendon and surrounding tissues in nine cadavers. Using MRI, we quantitatively evaluated each tissue from the horizontal plane in 40 healthy ankles. Macroscopic autopsy revealed the presence of adipose tissue behind the ankle joint between the FHL and fibula, and horizontal cross-sections showed an oval-shaped adipose tissue surrounding the tendon. The cross-sectional area on MRI was 14.4 mm<sup>2</sup> (11.7–16.7) for the FHL tendon and 120.5 mm<sup>2</sup> (100.3–149.4) for the adipose tissue. Additionally, the volume of the adipose tissue was 963.3 mm<sup>3</sup> (896.2–1115.6). There is an adipose tissue around FHL tendon and maybe this close anatomical relationship might influence the function of the tendon and be involved in its pathologies.

**Keywords** Flexor hallucis longus tendon, Talocrural joint, Adipose tissue

### Abbreviations

FHL Flexor hallucis longus  
MRI Magnetic resonance imaging  
CSA Cross-sectional area

Adipose tissue, which are present around tendons, plays a role in reducing friction and compressive stress<sup>1,2</sup>. In addition, adipose tissue contains nerve endings that serve the nociceptive function of tendons<sup>1,3,4</sup>. Moreover, because adipose tissue surrounding tendons also moves with tendon and joint movement<sup>5</sup>, decreased mobility of adipose tissue may cause tendinopathy and postoperative pain<sup>6,7</sup>. Pingel et al.<sup>8</sup> reported that changes in gene expression in samples of Achilles tendonitis patients were more consistent with inflammation of Kager's fat pad than healthy controls, suggesting that adipose tissue is involved in the pathogenesis. Therefore, adipose tissue is one of the important tissues for understanding the pathogenesis of tendinopathy<sup>8</sup>, and it is necessary to determine adipose tissue distribution for treatment in the field of rehabilitation and orthopedics.

The flexor hallucis longus (FHL) originates at the distal two-thirds of the posterior fibula and interosseous membrane of the lower leg, transitions into a tendon at the distal tibia, passes through the fibro-osseous tunnel, changes direction with the sustentacular tail, and courses towards the base of the great toe distal phalanx<sup>9,10</sup>. Tendon disorders of the FHL muscle reportedly occur in the between the fibro-osseous tunnel<sup>11</sup>, the great toe sesamoid<sup>11</sup>, at the junction of the tendon of the flexor digitorum longus<sup>12</sup> and the base of the great toe phalanx<sup>13</sup>. Particularly, disorders occur more frequently between the fibro-osseous tunnel and great toe sesamoid because of the poorer blood flow to the FHL tendon than that in other regions, considerable changes in the course of the tendon, and the application of excessive stress<sup>11</sup>. Although the affected area is more distal to the ankle joint, some patients experience posteromedial ankle pain after an ankle injury<sup>14,15</sup>. Furthermore, previous studies using magnetic resonance imaging (MRI) reported that some cases of pain around the FHL tendon after ankle trauma showed scarring of the surrounding tissue<sup>16</sup>. Although adipose tissue may also be present around the FHL tendon, its detailed anatomical structure remains unclear. Combined examination using gross anatomy and MRI has been performed for anatomical observations of adipose tissue<sup>17–19</sup>.

<sup>1</sup>Graduate School of Sports and Health Science, Ritsumeikan University, Shiga, Japan. <sup>2</sup>Department of Rehabilitation, Nagoya Sports Medicine & Orthopedic Clinic, Aichi, Japan. <sup>3</sup>College of Sport and Health Science, Ritsumeikan University, Shiga, Japan. <sup>4</sup>Research Organization of Science and Technology, Ritsumeikan University, Shiga, Japan. <sup>5</sup>Musculoskeletal Functional Anatomy Research Institute, Gifu, Japan. <sup>6</sup>Department of Orthopedic Surgery, Nagoya Sports Medicine & Orthopedic Clinic, Aichi, Japan. ✉email: yrs15159@fc.ritsumei.ac.jp

This study aimed to investigate the presence of adipose tissue surrounding the FHL tendon through gross dissection and MRI.

## Materials and methods

### Gross anatomical examination

Subjects for systematic dissection included nine cadavers and nine feet (average age:  $86.8 \pm 3.2$  years; 4 men, 5 women; 5 left feet, 4 right feet). To determine the structure of the FHL tendons and surrounding tissues, patients with a history of trauma, including fractures around the ankle and soft tissue injuries, were excluded.

An autopsy was carefully performed while inspecting each tissue to identify the FHL tendon and surrounding structures behind the ankle. The same procedure was performed by the same examiner for all cadavers.

First, the skin and subcutaneous adipose tissue were removed from the posterior ankle joint. The Achilles tendon and the Kager's fat pad were exposed distally to observe the relationship and boundary between the deep FHL tendon and surrounding tissue and the Kager's fat pad. To observe the positional relationship between the FHL tendon and surrounding tissues, we identified and removed the long and short peroneus, tibialis posterior, tibial nerve, and tibial posterior artery. Subsequently, the trochlea of the talus was used as an indicator to traverse the FHL tendon and surrounding tissues, which were also observed in the horizontal plane. Morphometry was performed using a digital caliper (SCALE-BK-150-MM, Waves, JAPAN) to measure the long and short axes of the FHL tendon and surrounding tissues at the level of the talar trochlea. Each measurement was performed three times, and the average value was used in all analyses. The intra-rater reliability of the FHL tendon and surrounding tissue measurements was verified by intraclass-correlation-coefficient (ICC), and the major axes ( $ICC = 0.88\text{--}0.98$ ) and minor axes ( $ICC = 0.97\text{--}0.98$ ) of the FHL tendon and major axes ( $ICC = 0.95\text{--}0.99$ ) and minor axes ( $ICC = 0.88\text{--}0.98$ ) for surrounding tissue were excellent, respectively.

### MRI study

A total of 40 feet from 20 healthy adults (12 men and 8 women; mean age,  $22.3 \pm 1.0$  years) were examined. Patients with a history of fracture around the FHL tendon, those with tendon disorders of the ankle joint, and those with significant limitation of range of motion or pain in the ankle joint were excluded. The study design was approved by the ethics committee of Ritsumeikan University (BKC—LSMH—2021—033), and all procedures were performed in accordance with the Declaration of Helsinki (last modified in 2013) and the Japanese guideline entitled, "Ethical Guidelines for Medical and Health Research Involving Human Subjects." All participants provided written informed consent.

#### *Morphometry of the FHL tendon and surrounding adipose tissues*

Using a 3.0-T MRI scanner (MAGNETOM Skyra; Siemens Healthineers, Japan), the patients were laid in a supine position with their knees extended and their legs parallel to the long axis of the gantry; the ankles were fixed in the plantar–dorsiflexed neutral position. T1-weighted spin echo images were captured using body coils with a matrix of  $512 \times 512$ , field-of-view of 350 mm, TR/TE of 700/8.8 ms, flip angle of  $120^\circ$ , and with no gap at 3-mm intervals from the distal lower leg to the calcaneus, focusing on the height where the FHL and soleus muscles meet. FHL tendons and surrounding adipose tissue were identified from the horizontal plane. After observing the positional relationship of each tissue, they were traced with reference to a slice of the trochlea of the talus, and their cross-sectional area (CSA) and volume were measured. The volume was calculated by adding all measured CSAs and multiplying them by the slice thickness (3 mm)<sup>20</sup>. Observations and measurements were quantitatively evaluated using Horos ver. 4.0 (Horos Project, USA).

#### *Relationship between morphometrics and physical characteristics of patients*

We investigated the influence of the physical characteristics of the patients on the morphometrics of the surrounding adipose tissue of the FHL tendon. Patients' characteristics, including body height, body weight, body mass index, lower leg length, and foot length, were measured, and the relationship between sex, left–right comparisons, and basic characteristics in each of the surrounding adipose tissue were assessed.

#### *Examining the positional relationship between the FHL tendon and surrounding adipose tissue*

The location of adipose tissue around the FHL tendon relative to the tendon around the ankle joint was examined. Based on the slice level of the trochlea of the talus, a straight line passing through the center of the talus and center of the Achilles tendon was defined as the y-axis, and the line perpendicular to the y-axis passing through the maximum bulge of the lateral malleolus was defined as the x-axis, with an intersection point at the origin (0, 0) (Fig. 1). Positive values were defined as lateral or posterior, whereas negative values were defined as medial or anterior.

Thereafter, we measured the coordinate centers of the FHL tendon and surrounding reference adipose tissue, the Achilles tendon, peroneal tendon, and tibialis posterior tendon to confirm their positional relationships. The coordinate center was measured using ImageJ software (v.1.53, National Institutes of Health, USA, <https://imagej.net/ij/index.html>).

## Statistical analysis

The relationship between height, weight, lower leg length, and foot length in each value of the surrounding adipose tissue was examined using Spearman's correlation coefficient, and the Mann–Whitney U test was used for sex- and left–right side-based comparisons. SPSS Statistics 20.0 (IBM, USA) was used for all analyses, with significance set at  $< 5\%$ .

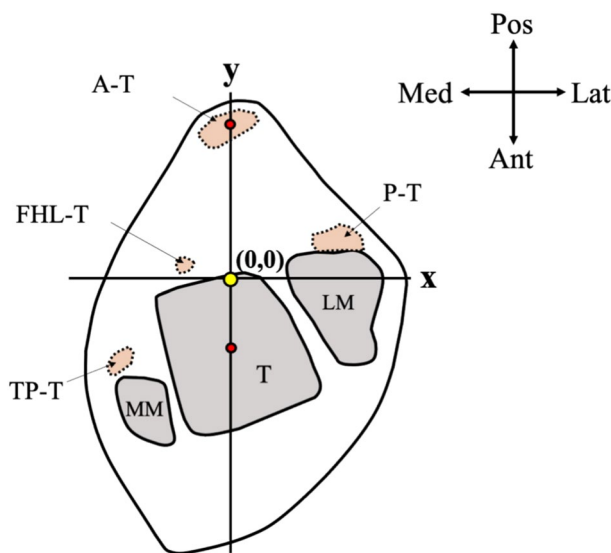


**Figure 1.** Coordinate axis settings. X-axis: Straight line to the Y-axis through the maximum bulge of the lateral malleolus. Y-axis: Straight line through the center of the talus and center of the Achilles tendon. Red circle: each center point; yellow circle: origin. FHL-T, flexor hallucis longus tendon; A-T, Achilles tendon; P-T, peroneal tendon; TP-T, tibialis posterior tendon; T, talus, MM, medial malleolus; LM, lateral malleolus; Pos, posterior; Ant, anterior; Lat, lateral, Med: medial.

### Ethical approval

This study was conducted after obtaining prior approval from the Ritsumeikan University Ethics Review Committee (BKC—LSMH—2021—033).

## Results

### Gross anatomical examination

In the posterior ankle joint, adipose tissue was observed between the FHL tendon, fibula, and lower lateral malleolus in all nine feet (Fig. 2a). Transverse observation of the FHL tendon and adipose tissue from a horizontal plane using the trochlea of the talus as a reference point revealed oval-shaped adipose tissue surrounding the tendon; the deep (anterior) layer was in contact with the posterior articular capsule and ligament of the talocrural joint (Fig. 2b), and this tissue could be clearly distinguished from Kager's fat pad, which is a single layer of adipose tissue located in the superficial layer (posterior) of the FHL tendon (Fig. 3).

Horizontal cross-section morphometry of the FHL tendon and surrounding adipose tissue revealed mean dimensions of  $6.3 \pm 0.8$  mm and  $3.2 \pm 0.5$  mm in the major and minor axes, respectively, for the FHL tendon and  $22.1 \pm 1.3$  mm and  $7.6 \pm 2.2$  mm in the major and minor axes, respectively, for adipose tissue (Fig. 4).

### MRI study

#### *Observation and morphometry of the FHL tendon and surrounding adipose tissue*

On axial MRI images (horizontal plane), the FHL tendon at the level of the talocrural joint in all 40 feet was surrounded by oval-shaped adipose tissues, while the ligament and posterior articular capsule of the talocrural joint were in the deep layer (Fig. 5). When the CSAs of the FHL tendon and adipose tissue were measured using the trochlea of the talus as an index, the median CSA of the FHL tendon was  $14.4 \text{ mm}^2$  ( $11.7$ – $16.7 \text{ mm}^2$ ) and that of the adipose tissue was  $120.5 \text{ mm}^2$  ( $100.3$ – $149.4 \text{ mm}^2$ ) (Fig. 6). Furthermore, the median volume of adipose tissue was  $963.3 \text{ mm}^3$  ( $896.2$ – $1115.6 \text{ mm}^3$ ).

#### *Relationship between morphometrics of adipose tissue surrounding the FHL tendon and physical characteristics of the patients*

Data on the physical characteristics of all patients are presented in Table 1.

The CSA of the adipose tissue demonstrated positive correlation with body height ( $r = 0.60$ ), body weight ( $r = 0.62$ ), body mass index ( $r = 0.50$ ), lower leg length ( $r = 0.40$ ), and foot length ( $r = 0.57$ ) of the patients. Additionally, the adipose tissue volume demonstrated positive correlation with body height ( $r = 0.66$ ), body weight ( $r = 0.63$ ), body mass index ( $r = 0.40$ ), lower leg length ( $r = 0.48$ ), and foot length ( $r = 0.63$ ) (Table 2).

The CSA and volume of the adipose tissue were significantly greater in men than those in women ( $p < 0.05$ ) (Fig. 7). However, no significant difference was observed between the left and right feet ( $p > 0.05$ ) (Fig. 8).

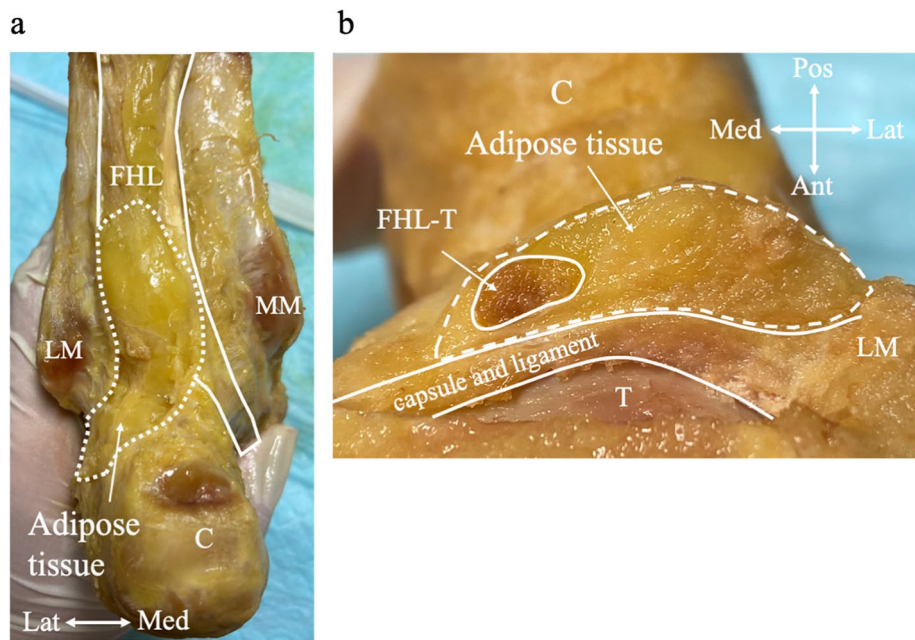


**Figure 2.** Adipose tissue surrounding the flexor hallucis longus tendon. **(a)** Adipose tissue surrounding the flexor hallucis longus tendon of the left ankle joint (posterior view). **(b)** Adipose tissue surrounding the flexor hallucis longus tendon at the level of the talocrural joint (horizontal). Dotted line: contour of adipose tissue. FHL-T, flexor hallucis longus tendon; T, talus; C, calcaneus; MM, medial malleolus; LM, lateral malleolus; Pos, posterior; Ant, anterior; Lat, lateral; Med, medial.

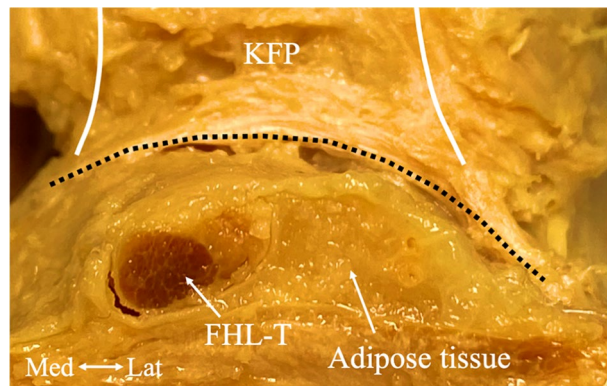


**Figure 3.** Border between adipose tissue surrounding the flexor hallucis longus tendon and superficial Kager's fat pad. Black dotted line: boundary with Kager's fat pad. FHL-T, flexor hallucis longus tendon; KFP, Kager's fat pad; Lat, lateral; Med, medial.

#### *Positional relationship between the FHL tendon and surrounding adipose tissues*

The coordinate centers ( $x, y$ ) of the FHL tendon, adipose tissue, Achilles tendon, peroneal tendon, and tibialis posterior tendon are presented in Table 3. Additionally, the coordinate center of the adipose tissue surrounding the FHL tendon was located at a level ( $y$  value) similar to that of the peroneus tendon (Fig. 9).

#### Discussion

This study aimed to evaluate the presence of adipose tissue surrounding the FHL tendon through anatomical observations and MRI findings. The clarification of these structures aims to enhance our understanding of diseases, guiding treatment selection for post-traumatic posteromedial ankle pain, such as ankle sprains and fractures, encountered in clinical practice.

In gross posterior view of the ankle, adipose tissue was present in the gap between the FHL tendon and fibula, while horizontal section of the talocrural joint revealed oval-shaped adipose tissue surrounding the FHL tendon. Although the FHL part of Kager's fat pad is in the superficial layer<sup>5</sup> of the FHL tendon, the boundary of each tissue was clearly demarcated from the ligament, suggesting that the adipose tissue surrounding the FHL

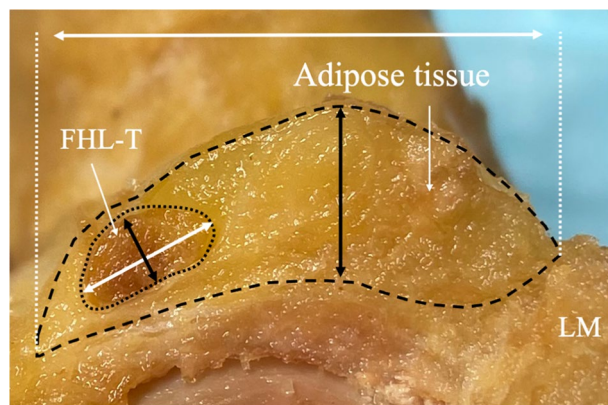


**Figure 4.** Methods for measuring the major and minor axes of the flexor hallucis longus tendon and surrounding adipose tissue. The maximum width of each tissue was defined as the major axes, and the maximum length was defined as the minor axes. White double arrows: major axes; black double arrows: minor axes. FHL-T, flexor hallucis longus tendon; LM, lateral malleolus.

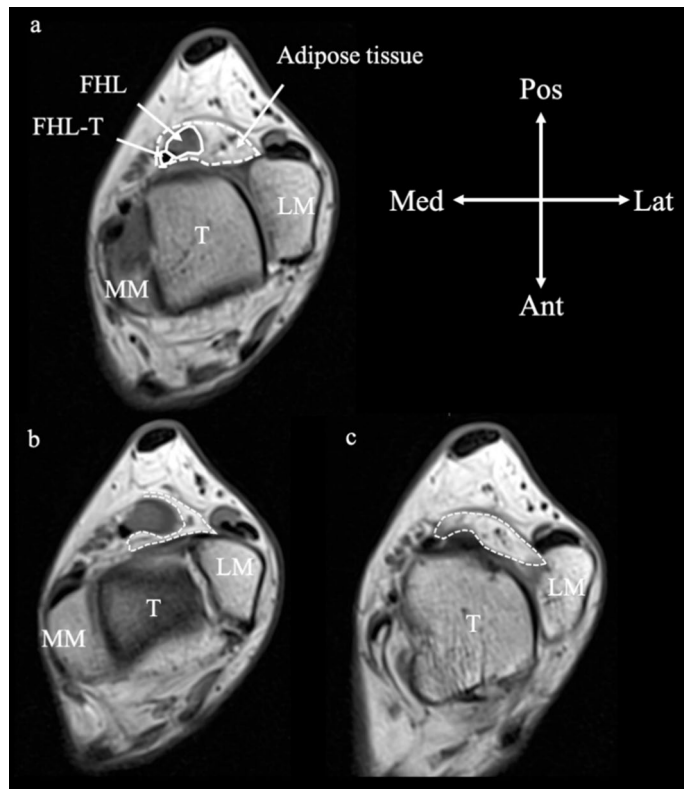


**Figure 5.** Magnetic resonance image of adipose tissue surrounding the flexor hallucis longus tendon. (a) At the level of the trochlea of the talus. (b) One slice proximal to the trochlea of the talus. (c) One slice distal to the trochlea of the talus. Dotted line: contour of adipose tissue. FHL, flexor hallucis longus; FHL-T, flexor hallucis longus tendon; T, talus; MM, medial malleolus; LM, lateral malleolus; Pos, posterior; Ant, anterior; Lat, lateral; Med, medial.

tendon is different from Kager's fat pad. However, since these boundaries were not observed histologically in this study, further investigation is necessary.

Morphometric analysis indicated that the volume of the adipose tissue surrounding the FHL tendon was  $963.3 \text{ mm}^3$  (median:  $896.2\text{--}1115.6 \text{ mm}^3$ ). Malagelada et al.<sup>21</sup> reported that the volume of Kager's fat pad to be  $10.6 \text{ mL}$  ( $10.600 \text{ mm}^3$ ) using the Archimedean principles from cadaver dissection. The measurement of tissue volume using MRI in this study has also been validated in previous studies<sup>22,23</sup>, and the volume of the adipose tissue surrounding the FHL tendon measured in this study was approximately 1/10 the size of Kager's fat pad.

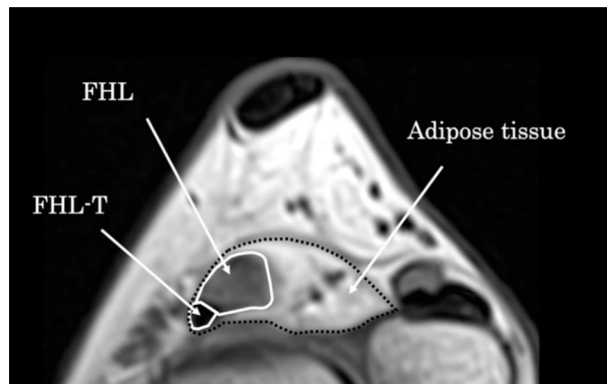


**Figure 6.** Method of measuring the cross-sectional area of adipose tissue around the flexor hallucis longus tendon. The cross-sectional area of adipose tissue was defined as the difference between the cross-sectional area of the flexor hallucis longus muscle and that of adipose tissue. Black dotted line: adipose tissue trace section. White line: flexor hallucis longus trace section. FHL, flexor hallucis longus; FHL-T, flexor hallucis longus tendon.

	Men n = 12 (24 feet)	Women n = 8 (16 feet)	Total n = 20 (40 feet)
Age (y)	23.0 (21.0–23.0)	23.0 (22.5–23.0)	23.0 (21.0–23.0)
Body height (cm)	175.5 (169.9–179.9)	161.8 (158.7–164.7)	168.3 (164.2–175.6)
Body weight (kg)	71.7 (63.3–76.0)	58.4 (54.3–60.0)	63.3 (58.4–73.6)
BMI (kg/m <sup>2</sup> )	22.2 (21.5–24.2)	21.6 (21.1–23.2)	22.2 (21.2–23.5)
Leg length (cm)	37.7 (36.3–40.0)	34.5 (34.0–36.1)	36.4 (35.2–38.0)
Foot Length (cm)	25.8 (24.8–26.5)	22.8 (22.2–23.5)	24.2 (23.0–26.0)

**Table 1.** Patients' physical characteristics. Y, years; cm, centimeter; Kg, kilogram; BMI, body mass index.

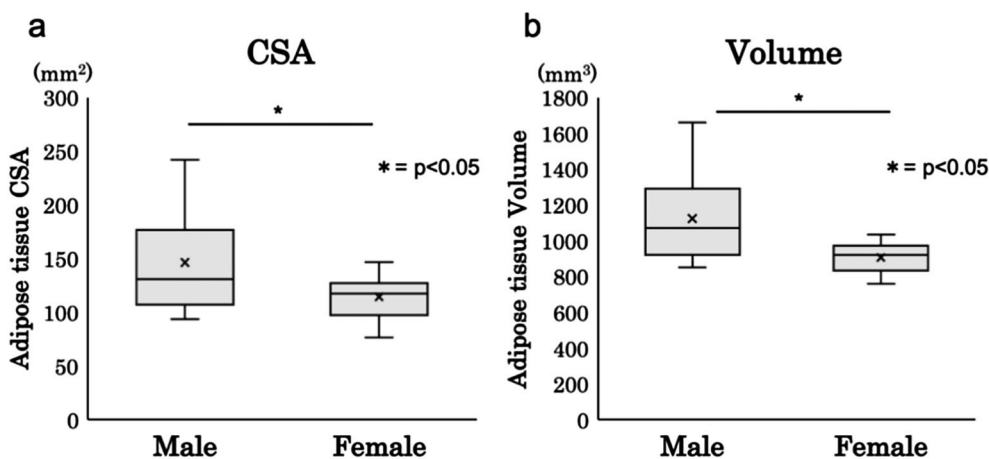
(a) Relationship between the cross-sectional area of adipose tissue and physical characteristics		
Adipose tissue CSA	r value	p value
Body height (cm)	0.60	<0.05
Body weight (kg)	0.62	<0.05
BMI (kg/m <sup>2</sup> )	0.50	<0.05
Leg length (cm)	0.40	<0.05
Foot Length (cm)	0.57	<0.05

(b) Relationship between the volume of adipose tissue and physical characteristics		
Adipose tissue Volume	r value	p value
Body height (cm)	0.66	<0.05
Body weight (kg)	0.63	<0.05
BMI (kg/m <sup>2</sup> )	0.40	<0.05
Leg length (cm)	0.48	<0.05
Foot Length (cm)	0.63	<0.05

**Table 2.** Relationship between the cross-sectional area and volume of adipose tissue and patients' physical characteristics. CSA, cross-sectional area; cm, centimeter; Kg, kilogram; BMI, body mass index.

Additionally, when the relationship between the adipose tissue CSA and volume and physical characteristics of patients was examined, a positive correlation was observed between each physical characteristic, which was significantly greater in men than in women. Patel et al.<sup>24</sup> examined the relationship between the FHL tendon and physical characteristics of patients using B-mode ultrasound and reported a positive correlation between the tendon form and foot length. Rosso et al.<sup>25</sup> examined the sex-based differences in the Achilles tendon length



**Figure 7.** Cross-sectional area and volume of adipose tissue by gender. (a) Adipose tissue cross-sectional area by gender. (b) Adipose tissue volume by gender. CSA, cross-sectional area.

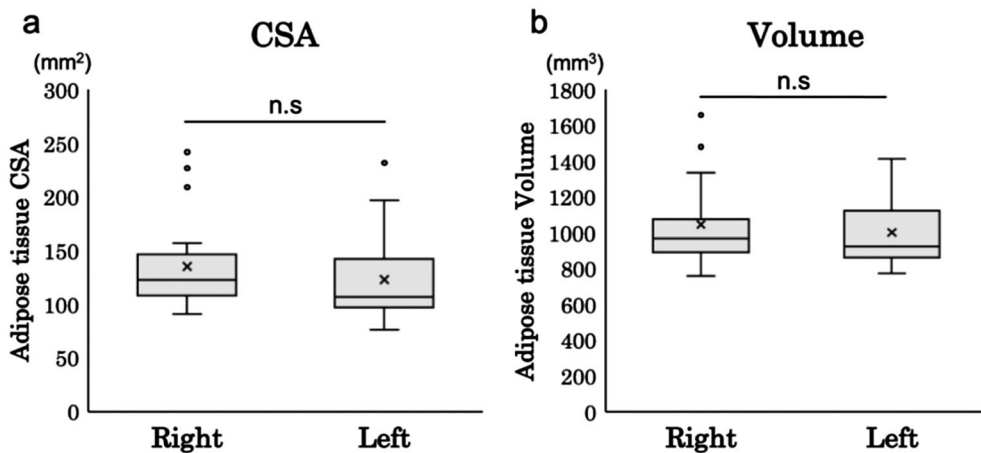


**Figure 8.** Left-right comparison of cross-sectional area and volume of adipose tissue. (a) Left-right adipose tissue cross-sectional area. (b) Left-right adipose tissue volume. CSA, cross-sectional area.

	FHL-T	Adipose tissue	A-T	P-T	TP-T
x value	$-6.8 \pm 1.9$	$3.5 \pm 1.3$	$0.2 \pm 0.7$	$25.5 \pm 2.3$	$-23.2 \pm 2.4$
y value	$7.9 \pm 3.0$	$9.7 \pm 2.4$	$32.1 \pm 3.5$	$9.0 \pm 2.3$	$-9.0 \pm 2.7$

**Table 3.** Mean value of the center of coordinates in each tissue (mm). Each value (x, y) represents the distance (mm) from the origin (0,0). FHL-T, flexor hallucis longus tendon; A-T, Achilles tendon; P-T, peroneal tendon; TP-T, tibialis posterior tendon.

and its relationship with lower leg length and body height using MRI and reported that the Achilles tendon length was significantly longer in men than in women, demonstrating a positive correlation with lower leg length and body height. Furthermore, a report investigating the relationship between the form of the intrinsic foot muscles, including their CSA and thickness, and physical characteristics using ultrasound imaging showed a positive correlation between the form of the intrinsic foot muscles and body height, body weight, foot length, and arch height<sup>26</sup>. Thus, it can be said that the size of organs and tissues constituting the body, such as muscles, tendons, and adipose tissues, is proportional to the body size. Similarly, the CSA and volume of adipose tissue is positively correlated with the physical characteristics, suggesting that the morphology of adipose tissue may be influenced by body size.

The adipose tissue around the tendon of the lower limbs is represented by Kager's fat pad<sup>5,21,27</sup> around the Achilles tendon and infrapatellar fat pad<sup>28,29</sup> around the patellar tendon. Adipose tissue not only serves as a buffer

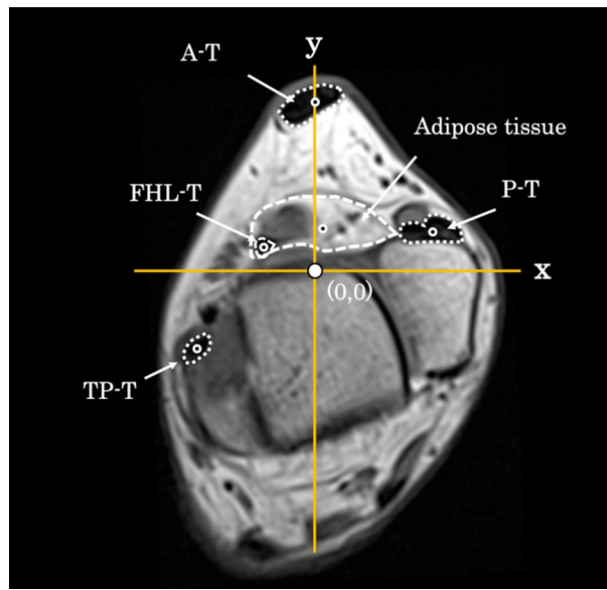


**Figure 9.** Coordinate center of each tissue. White circle: origin. Black circle: coordinate center of each tissue. FHL-T, flexor hallucis longus tendon; A-T, Achilles tendon; P-T, peroneal tendon, TP-T, tibialis posterior tendon.

to avoid direct collision between the tendon/ligament and bone<sup>21,30</sup> but also has proprioceptive and nociceptive functions for the tendon<sup>1,3</sup> because of the presence of nerve endings and neuro-related proteins.

Adipose tissue surrounding the FHL tendons may also be involved in the function and diseases of FHL tendons. However, the results of this study are insufficient to clarify the function of adipose tissue on FHL tendons or the involvement of adipose tissue in the disease. Therefore, further evaluation is needed on this topic.

## Conclusions

We evaluated the presence of surrounding adipose tissue in the FHL tendon through gross dissection and MRI examination. Adipose tissue, which is different from Kager's fat pad around the adjacent Achilles tendon, was observed around the FHL tendon.

## Data availability

The data that support the findings of this study will be available from the corresponding author upon reasonable request.

Received: 9 May 2024; Accepted: 16 July 2024

Published online: 23 July 2024

## References

1. Benjamin, M. *et al.* Adipose tissue at enthesis: The rheumatological implications of its distribution. A potential site of pain and stress dissipation?. *Ann. Rheum. Dis.* **63**(12), 1549–1555. <https://doi.org/10.1136/ard.2003.019182> (2004).
2. Clavert, P., Dosch, J. C., Wolfram-Gabel, R. & Kahn, J. L. New findings on intermetacarpal fat pads: Anatomy and imaging. *Surg. Radiol. Anat.* **28**(4), 351–354. <https://doi.org/10.1007/s00276-006-0106-z> (2006).
3. Shaw, H. M., Santer, R. M., Watson, A. H. & Benjamin, M. Adipose tissue at enthesis: The innervations and cell composition of the retromalleolar fat pad associated with the rat Achilles tendon. *J. Anat.* **211**(4), 436–443. <https://doi.org/10.1111/j.1469-7580.2007.00791.x> (2007).
4. Abreu, M. R., Chung, C. B., Trudell, D. & Resnick, D. Hoffa's fat pad injuries and their relationship with anterior cruciate ligament tears: New observations based on MR imaging in patients and MR imaging and anatomic correlation in cadavers. *Skelet. Radiol.* **37**(4), 301–306. <https://doi.org/10.1007/s00256-007-0427-y> (2008).
5. Theobald, P. *et al.* The functional anatomy of Kager's fat pad in relation to retrocalcaneal problems and other hindfoot disorders. *J. Anat.* **208**(1), 91–97. <https://doi.org/10.1111/j.1469-7580.2006.00510.x> (2006).
6. He, L., Genin, J. & Delzell, P. Ultrasound diagnosis and percutaneous treatment of Achilles tendon tethering: A case series. *Skelet. Radiol.* **45**(9), 1293–1298. <https://doi.org/10.1007/s00256-016-2416-5> (2016).
7. Hannon, J., Bardenett, S., Singleton, S. & Garrison, J. C. Evaluation, treatment, and rehabilitation implications of the infrapatellar fat pad. *Sports Health* **8**(2), 167–171. <https://doi.org/10.1177/1941738115611413> (2016).
8. Pingel, J. *et al.* Inflammatory and metabolic alterations of Kager's fat pad in chronic Achilles tendinopathy. *PLOS ONE* **10**(5), e0127811. <https://doi.org/10.1371/journal.pone.0127811> (2015).
9. Michelson, J. & Dunn, L. Tenosynovitis of the flexor hallucis longus: A clinical study of the spectrum of presentation and treatment. *Foot Ankle Int.* **26**(4), 291–303. <https://doi.org/10.1177/107110070502600405> (2005).
10. Theodoropoulos, J. S., Wolin, P. M. & Taylor, D. W. Arthroscopic release of flexor hallucis longus tendon using modified posteromedial and posterolateral portals in the supine position. *Foot (Edinb.)* **19**(4), 218–221. <https://doi.org/10.1016/j.foot.2009.02.002> (2009).

11. Petersen, W., Pufe, T., Zantop, T. & Paulsen, F. Blood supply of the flexor hallucis longus tendon with regard to dancer's tendinitis: Injection and immunohistochemical studies of cadaver tendons. *Foot Ankle Int.* **24**(8), 591–596. <https://doi.org/10.1177/107100700302400804> (2003).
12. Wei, S. Y., Kneeland, J. B. & Okereke, E. Complete atraumatic rupture of the flexor hallucis longus tendon: A case report and review of the literature. *Foot Ankle Int.* **19**(7), 472–474. <https://doi.org/10.1177/107110079801900709> (1998).
13. Krackow, K. A. Acute, traumatic rupture of a flexor hallucis longus tendon: A case report. *Clin. Orthop. Relat. Res.* **150**, 261–262. <https://doi.org/10.1097/00003086-198007000-00044> (1980).
14. Liu, S. H. & Mirzayan, R. Posteromedial ankle impingement. *Arthroscopy* **9**(6), 709–711. [https://doi.org/10.1016/s0749-8063\(05\)80514-6](https://doi.org/10.1016/s0749-8063(05)80514-6) (1993).
15. Lui, T. H. Endoscopic adhesiolysis of the flexor hallucis longus muscle. *Foot Ankle Spec.* **7**(6), 492–494. <https://doi.org/10.1177/1938640014546859> (2014).
16. Lo, L. D. *et al.* MR imaging findings of entrapment of the flexor hallucis longus tendon. *AJR* **176**(5), 1145–1148. <https://doi.org/10.2214/ajr.176.5.1761145> (2001).
17. Staebli, H. U., Bollmann, C., Kreutz, R., Becker, W. & Rauschning, W. Quantification of intact quadriceps tendon, quadriceps tendon insertion, and suprapatellar fat pad: MR arthrography, anatomy, and cryosections in the sagittal plane. *AJR Am. J. Roentgenol.* **173**(3), 691–698. <https://doi.org/10.2214/ajr.173.3.10470905> (1999).
18. Skaf, A. Y. *et al.* Pericruciate fat pad of the knee: Anatomy and pericruciate fat pad inflammation: Cadaveric and clinical study emphasizing MR imaging. *Skelet. Radiol.* **41**(12), 1591–1596. <https://doi.org/10.1007/s00256-012-1447-9> (2012).
19. Takumi, O. *et al.* Presence of adipose tissue along the posteromedial tibial border. *J. Exp. Orthop.* **8**(1), 92. <https://doi.org/10.1186/s40634-021-00408-0> (2021).
20. Kusagawa, Y. *et al.* Associations between the size of individual plantar intrinsic and extrinsic foot muscles and toe flexor strength. *J. Foot Ankle Res.* **15**(1), 22. <https://doi.org/10.1186/s13047-022-00532-9> (2022).
21. Malagelada, F. *et al.* Pressure changes in the Kager fat pad at the extremes of ankle motion suggest a potential role in Achilles tendinopathy. *Knee Surg. Sports Traumatol. Arthrosc.* **28**(1), 148–154. <https://doi.org/10.1007/s00167-019-05585-1> (2020).
22. Culvenor, A. G., Cook, J. L., Warden, S. J. & Crossley, K. M. Infrapatellar fat pad size, but not patellar alignment, is associated with patellar tendinopathy. *Scand. Med. Sci. Sports* **21**(6), 405–411. <https://doi.org/10.1111/j.1600-0838.2011.01334.x> (2011).
23. van der Heijden, R. A. *et al.* Quantitative volume and dynamic contrast-enhanced MRI derived perfusion of the infrapatellar fat pad in patellofemoral pain. *Quant. Imaging Med. Surg.* **11**(1), 133–142. <https://doi.org/10.21037/qims-20-441> (2021).
24. Patel, N. N. & Labib, S. A. The Achilles tendon in healthy subjects: An anthropometric and ultrasound mapping study. *J. Foot Ankle Surg.* **57**(2), 285–288. <https://doi.org/10.1053/j.jfas.2017.10.005> (2018).
25. Rosso, C. *et al.* Physiological Achilles tendon length and its relation to tibia length. *Clin. J. Sport Med.* **22**(6), 483–487. <https://doi.org/10.1097/JSM.0b013e3182639a3e> (2012).
26. Franettovich Smith, M. M., Hides, J. A., Hodges, P. W. & Collins, N. J. Intrinsic foot muscle size can be measured reliably in weight bearing using ultrasound imaging. *Gait Posture* **68**, 369–374. <https://doi.org/10.1016/j.gaitpost.2018.12.012> (2019).
27. Goodman, L. R. & Shanser, J. D. The pre-Achilles fat pad: An aid to early diagnosis of local or systemic disease. *Skelet. Radiol.* **2**, 81–86. <https://doi.org/10.1007/BF00360986> (1977).
28. Saddik, D., McNally, E. G. & Richardson, M. MRI of Hoffa's fat pad. *Skelet. Radiol.* **33**(8), 433–444. <https://doi.org/10.1007/s00256-003-0724-z> (2004).
29. Gallagher, J., Tierney, P., Murray, P. & O'Brien, M. The infrapatellar fat pad: Anatomy and clinical correlations. *Knee Surg. Sports Traumatol. Arthrosc.* **13**(4), 268–272. <https://doi.org/10.1007/s00167-004-0592-7> (2005).
30. Kuhns, J. G. Changes in elastic adipose tissue. *J. Bone Joint Surg. Am.* **31**(3), 541–547 (1949).

## Acknowledgements

The authors thank Editage (www.editage.com) for English language editing. In addition, the authors acknowledge and thank the anonymous individuals who generously donated their bodies in order for this study to be performed.

## Author contributions

The conception and design of the study were done by T. K. and Y. S. The acquisition of data was taken care of by T. K., T. K., H. S., K. I. Analysis and/or interpretation of data was carried out by T. K., T. K., H. S., K. I., M. F., and N. H. The drafting of the article was done by T. K., Y. S. and K. S. Revising the article critically for important intellectual content was taken care of by K. S. All authors have contributed significantly to the study, approved the article, and agreed with the submission.

## Funding

The authors did not receive support from any organization for the submitted work.

## Competing interests

The authors declare no competing interests.

## Additional information

Correspondence and requests for materials should be addressed to Y.S.

Reprints and permissions information is available at [www.nature.com/reprints](http://www.nature.com/reprints).

**Publisher's note** Springer Nature remains neutral with regard to jurisdictional claims in published maps and institutional affiliations.



**Open Access** This article is licensed under a Creative Commons Attribution-NonCommercial-NoDerivatives 4.0 International License, which permits any non-commercial use, sharing, distribution and reproduction in any medium or format, as long as you give appropriate credit to the original author(s) and the source, provide a link to the Creative Commons licence, and indicate if you modified the licensed material. You do not have permission under this licence to share adapted material derived from this article or parts of it. The images or other third party material in this article are included in the article's Creative Commons licence, unless indicated otherwise in a credit line to the material. If material is not included in the article's Creative Commons licence and your intended use is not permitted by statutory regulation or exceeds the permitted use, you will need to obtain permission directly from the copyright holder. To view a copy of this licence, visit <http://creativecommons.org/licenses/by-nc-nd/4.0/>.

© The Author(s) 2024